

# We are IntechOpen, the world's leading publisher of Open Access books Built by scientists, for scientists

6,900

Open access books available

186,000

International authors and editors

200M

Downloads

Our authors are among the

154

Countries delivered to

TOP 1%

most cited scientists

12.2%

Contributors from top 500 universities



WEB OF SCIENCE™

Selection of our books indexed in the Book Citation Index  
in Web of Science™ Core Collection (BKCI)

Interested in publishing with us?  
Contact [book.department@intechopen.com](mailto:book.department@intechopen.com)

Numbers displayed above are based on latest data collected.  
For more information visit [www.intechopen.com](http://www.intechopen.com)



# Nanoporous Oxides and Nanoporous Composites

*Dong Duan, Haiyang Wang, Wenyu Shi and Zhanbo Sun*

## Abstract

Nanoporous oxides, such as cupric oxide (CuO), nickelous oxide (NiO), titanium dioxide (TiO<sub>2</sub>), cobaltous oxide (Co<sub>3</sub>O<sub>4</sub>), and cerium oxide (CeO<sub>2</sub>), and noble-metal-based nanoporous composites, such as silver (Ag) ligaments loaded with CeO<sub>2</sub>, TiO<sub>2</sub>, zirconium dioxide (ZrO<sub>2</sub>) or NiO and palladium (Pd) ligaments loaded with TiO<sub>2</sub> or ZrO<sub>2</sub>, are described in the chapter. Oxide-based nanoporous composites, such as Au loaded on CuO and CeO<sub>2</sub> or platinum (Pt) loaded on TiO<sub>2</sub>, are also summarized. The structures, microstructures, and microstructure parameters of these materials are reviewed. The performance of the noble-based nanoporous composites is presented, including the catalytic oxidation of methanol and ethanol. Environmental protection applications, such as catalytic oxidation of carbon monoxide (CO) for the oxide-based nanoporous composites, have also been developed. Applications of rare earth elements in nanoporous materials are also reviewed.

**Keywords:** precursor alloy, dealloying, nanoporous oxides, nanoporous composites, rare earth elements

## 1. Introduction

Research on nanoporous materials prepared by dealloying originated from work with nanoporous noble metals. During dealloying, the active metals in precursor alloys composed of corrosion-resistant noble metals, such as Ag and gold (Au), and cheaper metals, such as manganese (Mn), zinc (Zn), aluminum (Al), and magnesium (Mg), were selectively removed. Simultaneously, ligaments of corrosion-resistant noble metals and pores were formed [1]. At the nanoscale, both the preparation and the performance of noble metals have unparalleled advantages due to the excellent catalytic activity and chemical stability. However, the high price and the scarce resources of noble metals have prompted investigation of new paths to reduce their usage, resulting in the formation of alloy nanoporous materials containing less noble metals [2].

Certain metals, such as copper (Cu), nickel (Ni), and cobalt (Co), can remain in dilute acid or alkali solutions and maintain acceptable catalytic properties. These metals are potential substitutes for noble metals. Therefore, the preparation of cheaper nanoporous metals, such as Cu, was investigated [3]. However, it was found that the nanoscale ligaments inevitably oxidized in air or corrosive media due to small scale and large surface effects after dealloying, which means that the materials must be kept in a special environment. These materials cannot be used in ideal

environmental conditions, which will inevitably lead to their limited use. Certain nanooxides, such as CuO, NiO, cobaltic oxide ( $\text{Co}_2\text{O}_3$ ), and  $\text{CeO}_2$ , have acceptable catalytic activities. In acid and alkali solutions, certain stable metals, such as Cu, Ni, and Co, can form nanoporous oxides after further oxidation [4–6]. These metals could be used to produce nanoporous composites with excellent catalytic performance after they are loaded with noble metals.

Research [7] has shown that the interface between the noble metal and loaded oxides and the interaction between the two phases can significantly enhance the catalytic activity at the nanoscale. Certain oxides, such as  $\text{CeO}_2$ , could prevent poisoning and failure of noble metals when loaded on the surface of noble metals. To improve the performance of noble metals, the proper amount of oxides should be loaded on the ligament surface of the noble metal. The direct solution mechanism is to infiltrate the target metal saline solution into the nanoporous metals. The metal ions are transformed into oxides after drying or dewatering. However, the added matter concentrates on the surface layer of the sample during drying of the aqueous solution, causing little oxide to be distributed in the inner region. In 2013, Li et al. added cerium (Ce) to the Al-Ag precursor alloy. With the removal of Al elements during corrosion, Ce compounds are formed during the formation of nanoporous Ag. After heat treatment in air or oxygen ( $\text{O}_2$ ),  $\text{CeO}_2$  is formed and loaded on the surface of Ag ligaments to create a nanoporous composite material of Ag ligament loaded with  $\text{CeO}_2$  [8]. This material's performance was significantly better than that of pure nanoporous Ag. Nanoporous Ag loaded with  $\text{TiO}_2$  [9] and  $\text{ZrO}_2$  [10] and nanoporous Pd loaded with NiO [11] and  $\text{TiO}_2$  [12] have also been prepared.

Certain metals, such as Ce and titanium (Ti), are active elements. However, they do not evolve into ions that are removed in alkaline solutions, such as sodium hydroxide (NaOH) and potassium hydroxide (KOH). Instead, they evolve into solid compounds containing water, and the nanoporous structure is formed after crystallization. Some of them, such as Ce and samarium (Sm), also form nanorods because the crystallization has a clear direction. After high-temperature dehydration, they evolved into rare earth oxide nanorods [5, 13]. The nanorods support each other and form a supporting pore structure or framework with a large number of pores. If noble metals, such as Au and Ag, are added to the precursor alloys in small quantities, the noble metal nanoparticles or atoms are loaded on the surface of the nanorods. These metals presented excellent gas catalytic activity [6, 14].

Focusing on the work of our group, this chapter introduces the recent development of nanoporous oxides and nanoporous composites prepared by dealloying. The design principle of the precursor alloys and preparation process and dealloying methods and effects of the preparation process on the morphologies and physical parameters of nanoporous oxides and nanoporous composites are reviewed.

## **2. Design and preparation of precursor alloys and the dealloying process**

Generally, the more active elements, that is, the elements removed by corrosion in the precursor alloys, are the higher the porosity of the nanoporous material is and the thinner the ligaments are after dealloying. However, if the stable metal content is too low, that is, less than 5 at%, the nanoporous structure may not form. Therefore, a stable metal content of 8–15 at% is recommended [4–14]. In addition, it is important to consider whether the components can form alloys. If the solubility between the components is not good in the melt, it is likely that the alloy will have a serious tendency to macrosegregate, and the ideal nanoporous structure cannot form after dealloying. Some systems, such as the Al-Ti system, have a large temperature difference between the liquidus and the solidus on the Al-rich side (when

10% Ti is used, the distance between liquidus and the solidus is approximately 585°C), which would result in a serious macrosegregation tendency. Therefore, the Ti content should be minimized if possible. Thus, a eutectic system, such as Al-Cu, is an ideal precursor alloy. For some systems, such as Al-Ce and Al-Pt systems, the temperature difference between the liquidus and solidus is not very large. The melt quenching can be used to prepare precursor alloys with homogeneous composition. In addition, systems with a little or no intermetallic compounds in the precursor alloys are suitable for preparing nanoporous materials by dealloying. Some intermetallic compounds, such as  $\text{Ag}_2\text{Al}$  in the Al-Ag system, do not effectively decompose in alkaline solutions at room temperature, resulting in residual  $\text{Ag}_2\text{Al}$  and decreased Ag content in the nanoporous structures [8–10]. The properties of the nanoporous structures were less optimal. Certain intermetallic compounds, such as  $\text{Al}_2\text{Cu}$ , easily decompose in corrosion fluids, and its content has little effect on nanostructures. If a binary alloy cannot form an ideal nanoporous material, a third component could be added to the binary system. However, the third component should be completely removed in the dealloying. For example, Li et al. added an appropriate amount of rare earth element Ce to Cu-Ag alloys, resulting in significant microstructure refinement of the precursor alloys [15]. After electrochemical dealloy removal in aqueous cupric sulfate ( $\text{CuSO}_4$ ), all of the Al and Ce were removed, and the microstructure of the nanoporous Ag was obviously refined.

For nanoporous oxides, binary precursor alloy systems, such as Al-Cu [3, 4], Al-Ni [5], and Al-Ce [5], can be used. For the noble metal-loaded oxide systems, Al-noble metal-oxide formation elements can be used to form ternary alloy systems, such as Al-Ag-Ce [8] and Al-Pd-Ni [11]. Their noble metal content is approximately 10–15%, and the oxide-forming element content is generally less than 2 at%. In the dealloying, elemental Al is dissolved or removed and the two other elements remain. Using components with higher noble metal content, noble metal would form ligaments. After heat treatment, oxide particles form and load on the surface of the ligaments. In oxide-loading noble metal systems, the precursor alloys are Al-oxide formation element-noble metal ternary systems, such as Al-Cu-Au [4], Al-Ce-Au [14], and Al-Ti-Pt [16]. Their oxide-formation element content is approximately 8–10%, and their noble metal content is less than 2%. In the dealloying, Cu, Ce, and Ti are oxidized into oxides and form ligaments. The noble metals are loaded on the surface of ligaments after forming nanoparticles.

Intermediate alloy ingots can be synthesized by melting and powder metallurgy. Melting is the most recommended method. However, the direct dealloying of alloy ingots results in a longer dealloying time due to their larger ingot size. The size of ligaments and holes might be too large. Some systems, such as Cu-Ag and Al-Cu systems, can be made into thin strips by cold rolling. However, other systems, such as the Al-Ti system, do not allow for creating a high-quality precursor by cold rolling due to poor ductility. Thus, it is necessary to adopt melt spinning. Melt spinning is a rapid solidification process. In this method, alloy melts can directly solidify or evolve into thin ribbons at cooling rates of  $10^6$ – $10^9$  K/s. Based on the conditions adopted, the thickness of the thin ribbons can be controlled from 20 to 100  $\mu\text{m}$ , and the width can be adjusted. For most alloys, alloy ribbons with a highly homogeneous distribution of elements can be obtained by melt spinning or melt quenching. Binary Al-Ti and Al-Ce and ternary Al-Ti-Pt and Al-Ce-Au systems could be prepared into high-quality precursor ribbons. If the required thin ribbons cannot be prepared in this manner, the system might not be an optimal precursor alloy for nanoporous materials.

Hydrochloric acid or aqueous KOH or NaOH is often used as dealloying solvents. The dealloying temperature should be room temperature. However, at higher temperatures such as 80°C, nanorod support pore structures can form [5, 6, 14] in the Al-Ce precursor system. Thus, the dealloying temperature is important for products



with specific morphologies. In dealloying, the smaller components in the precursor alloys are distributed in the ligaments by mechanical mixing. During subsequent heat treatment, the ligament begins to crystallize or crystallizes further. The loaded elements cannot be fixed or dissolved in the ligaments, and they are forced to diffuse to the surface of the ligament. This promotes the formation of nanoparticles and atomic load on the ligament surface. As a result, composite materials from loading the ligament surface with other particles evolve well [4]. Regardless of whether the noble metal is loaded on oxides or the oxides are loaded on noble metals, designing the proper composition of precursor alloys is critical. Notably, the binding between the load and the carrier in the nanoporous composite prepared by dealloying is similar to that of metallurgical binding or a semi-embedding structure [4]. Compared with other methods, they have a stronger binding force, which is conducive to the stability of structures and stronger interface effects.

Heat treatment or calcination is an indispensable procedure in preparation of nanoporous oxides and nanoporous composites. During heat treating, some elements are oxidized into oxides and the desired structures can be formed [4, 5, 8, 9, 13, 14]. In certain composites, such as  $\text{Co}_3\text{O}_4$  [17] and  $\text{CeO}_2$  loaded with Au [14], interface and crystalline defects occurred. This can be useful to enhance the catalytic properties. The calcination technologies indicated that the choice of atmosphere should be optimized according to the materials. This approach provides a starting point for researchers. However, certain composites, such as nanoporous Pd loaded with oxides [11, 12, 18], are not suitable for calcination because the nano Pd easily oxidizes at high temperatures.

Rare earth elements are important metallurgical additives in the industry. In the past 5 years, rare earth elements, such as Ce, have been used in research examining nanoporous materials [5, 6, 8, 14, 15]. The Ce in melt-spun Cu-Ag-Ce alloys can observably refine the microstructures of precursors. The nanoporous structures were obviously fine after electrochemistry dealloying, and all Cu and Ce were removed [15]. The most compounds with rare earth elements could be decomposed during dealloying. Some rare earth elements, such as lanthanum (La), Ce, neodymium (Nd), and Sm, could not be removed by NaOH and KOH solutions at up to  $100^\circ\text{C}$ . When their contents are lower, that is, less than 2%, they can be loaded by ligaments of noble metals, resulting in improved catalytic properties [8]. In alkali liquors, these elements can form compounds with water and crystallize. The crystallization has specific directions, which results in the formation of nanorods at temperatures above  $80^\circ\text{C}$ . The compounds with water can transform into rare earth oxidations after dehydration, and a framework structure constructed by support nanorods forms [5, 8, 14]. Rare earth oxidation nanorods are important carriers loaded by nobles and other oxidations because they have special interactions with other matter. The composites present excellent catalytic properties. In 5% nitric acid ( $\text{HNO}_3$ ) solution, the  $\text{CeO}_2$  can be removed. Ultrafine nanoporous Pt with excellent properties was also achieved [19].

### 3. Nanoporous oxides

Transition metal oxides (TMOs) are important nanoporous materials exhibiting a wide variety of structures and electronic and magnetic properties due to the nature of the outer d states [20]. Nanoscale transition metal oxides exhibit favorable catalytic activity for catalytic oxidation of harmful gases due to the presence of variable valency ions [21–23]. Transition metal oxide semiconductor materials, such as  $\text{TiO}_2$ , have important applications in photocatalytic hydrogen production and photodegradation due to their nontoxicity, high chemical stability, low cost,

and light stability [24–26]. Thus, research has been devoted to the creation of stable ordered nanoporous transition metal oxides.

### 3.1 Nanoporous CuO

In 2015, Zhang et al. reported that nanoporous CuO was prepared by a simple method of dealloying Al-Cu alloy ribbon in alkaline solution and calcining in air [4]. The precursor ingots were obtained by melting alloys composed of pure Al and pure Cu. The ribbons were prepared by melt spinning at  $33 \text{ m s}^{-1}$  and protected by 0.05 MPa argon (Ar). The as-quenched ribbons were immersed into aqueous 5 wt% NaOH at room temperature. The dealloyed ribbons were calcined at  $600^\circ\text{C}$  for 1 h in air. The results showed that the samples are mainly composed of Cu and copper (I) oxide ( $\text{Cu}_2\text{O}$ ) after dealloying and only CuO could be detected after calcination at  $600^\circ\text{C}$ . The prepared CuO exhibits a three-dimensional interpenetrating nanoporous structure with mesoporous properties. The pore size is approximately 25 nm, and the ligament size is approximately 50 nm. The materials have good redox capacity and can be used for the catalytic oxidation of CO. The reaction temperature for catalyzing 50% of CO is approximately  $170^\circ\text{C}$ , and the temperature for completely converting CO is  $240^\circ\text{C}$ . The long-term stability did not degrade even after 60 h, indicating that its performance is favorable.

In 2017, Li et al. reported the fabrication of a 3D free-standing CuO nanowire array supported by a nanoporous CuO network by dealloying  $\text{Cu}_{60}\text{Zr}_{35}\text{Al}_5$  glassy ribbons in a dilute HF aqueous solution at  $0.05 \text{ mol L}^{-1}$  for 12 h at room temperature [27]. The CuO nanocomposite exhibits a hierarchical nanostructure containing a well-aligned CuO nanowire array and nanoporous substrate with continuous nanoporosity. The nanoporous CuO exhibits superior degradation performance for methylene blue in the presence of hydrogen peroxide ( $\text{H}_2\text{O}_2$ ) compared to that of commercial CuO nanoparticles. The remarkable catalytic activity and good reusability and stability during degradation make the as-prepared nanocomposite a promising candidate for purifying wastewater with organic dyes. The high degradation efficiency of the nanocomposite mainly results from the uniform nanowire array structure and its high internal surface area, which provide more effective contact between the MB and catalysts [27].

### 3.2 Nanoporous NiO

In 2013, Liang et al. reported that a three-dimensional (3D) nanoporous NiO film was fabricated via a two-step process using an electrochemical route [28]. The dealloying process included electrodeposition of the Ni/Zn alloy film and electrochemical dealloying using a direct-current power source. The NiO film had an irregular 3D interconnected nanosheet structure with open channels. The specific capacitance of the NiO reached  $1670 \text{ F g}^{-1}$  at a discharge current density of  $1 \text{ A g}^{-1}$  for the supercapacitor. In addition, the NiO exhibited high performance during a long-term cycling. The maximum specific energy and specific power at the 1.1 V potential window were 170 and  $27.5 \text{ kW kg}^{-1}$ , respectively.

In 2016, Zhang et al. successfully prepared nanoporous NiO by dealloying  $\text{Al}_{85}\text{Ni}_{15}$  alloy and calcining in air [5]. The precursor alloys were prepared by similar methods with Al-Cu [4]. The surface and pores of the sample present a nanoporous structure. The pore diameter is approximately 30–50 nm, the pore walls are composed of island-like barriers, and the width is approximately 50 nm. The entire material presents a porous frame structure with a uniform pore size. It achieved good performance in the catalytic oxidation of CO, and the active temperature of fully catalyzed oxidation of CO was approximately  $340^\circ\text{C}$ .

### 3.3 Nanoporous $\text{Co}_3\text{O}_4$

In 2011, Xu et al. employed a simple fabrication method for  $\text{Co}_3\text{O}_4$  nanosheets through dealloying Al-Co alloy in alkaline solutions [17]. The precursor alloy was  $\text{Al}_{95}\text{Co}_5$ , and ribbons were prepared by melt spinning. The microstructure was a hierarchical flower-like aggregate structure with the typical size at the micron scale, where each nanoflower is composed of many irregular interlaced nanoslices with thicknesses as small as 6 nm, which is a typical porous structure. The results indicated that  $\text{Co}_3\text{O}_4$  nanosheets exhibited excellent catalytic activity for CO oxidation at ambient temperature, the reaction temperature for catalyzing 50% of the CO was approximately  $80^\circ\text{C}$ , and the temperature for completely converting the CO was  $140^\circ\text{C}$ . Calcination in an  $\text{O}_2$  atmosphere was essential to achieve high CO oxidation activity for these nanostructures, which allowed for the generation of active species for surface reactions. In addition, the calcination temperature significantly affected the catalytic activity;  $300^\circ\text{C}$  was a more favorable calcination temperature than  $200$  or  $450^\circ\text{C}$ , considering the optimum balance between the active reaction species and the surface area upon calcination. In addition,  $\text{Co}_3\text{O}_4$  nanosheets showed good time-onstream catalytic stability. It is expected that many other useful metal oxide materials can be fabricated similarly. Due to the evident advantages of simple processing, nearly perfect yield, and low fabrication cost, these functional nanomaterials may lead to applications in various catalytic processes.

### 3.4 Nanoporous $\text{TiO}_2$

In 2018, Shi et al. prepared nanoporous  $\text{TiO}_2$  by dealloying an Al-Si-Ti precursor alloy and calcining [16]. The  $\text{Al}_{61}\text{Si}_{30}\text{Ti}_9$  precursor alloy was prepared from pure Al, Ti, and silicon (Si) by arc-melting. The melt-spun ribbons were obtained by melt spinning at  $33 \text{ m s}^{-1}$  and protected by 0.05 MPa Ar. The as-quenched ribbons were dealloyed in aqueous 10% NaOH at  $80^\circ\text{C}$ . Subsequently, the ribbons were immersed in aqueous 3% (by weight) hydrogen chloride (HCl) at an ambient temperature for 7 h. The samples were then calcined at  $400^\circ\text{C}$  for 2 h. The results show that nanoporous  $\text{TiO}_2$  exhibits a laminated sheet morphology, and the irregular sheets show a pore-ligament structure. The structure had large specific surface areas, small pore diameters, and large pore volumes. The measurements also revealed that nanoporous  $\text{TiO}_2$  had favorable photocatalytic performance in degradation of methyl orange (MO).

### 3.5 Rare earth oxides

Due to the special electronic structure of rare earth elements, which have unique physical and chemical properties, and the continuous development of nanotechnology, the preparation of nanoporous rare earth oxides has attracted increasing attention [29, 30]. Rare earth oxides such as  $\text{CeO}_2$  have heterogeneous catalytic ability and excellent storage/deoxygenation capacity, which is optimal for supporting noble metal nanoparticle carriers [31, 32]. Nanoporous rare earth oxides have a wide range of applications in energy, chemical, environmental, and magnetic materials.

In 2017, Zhang et al. reported a  $\text{CeO}_2$  nanorod framework synthesized via dealloying Al-Ce alloys coupled with calcination treatment [5]. The precursor alloy was  $\text{Al}_{90}\text{Ce}_{10}$ , and ribbons were prepared by melt spinning at  $33 \text{ m s}^{-1}$  and protected by 0.05 MPa Ar. The precursor alloy ribbons were dealloyed in 20 wt% NaOH solution at  $80^\circ\text{C}$ . The dealloyed samples were heat treated at  $400^\circ\text{C}$  in  $\text{O}_2$ . After dealloying, the  $\text{CeO}_2$  particles grew into nanorods with a diameter of approximately 20 nm. The nanorods piled up into frameworks containing pores. The nanorods and pores were



homogeneously distributed and formed the framework structure. The material presented favorable CO catalytic oxidization properties: the reaction temperature for catalyzing 50% of CO was approximately 300°C, and the temperature for completely converting CO was 440°C. In 2018, Wang et al. reported that the CeO<sub>2</sub> nanorod framework also exhibits a high-specific capacitance and superior charge/discharge stability, which are mainly ascribed to its high-Brunauer-Emmett-Teller surface area [33].

In 2018, Duan et al. prepared nanorod samarium oxide (Sm<sub>2</sub>O<sub>3</sub>) by dealloying Al-Sm alloy and calcining in O<sub>2</sub> [13]. The preparation is the same as in the CeO<sub>2</sub> framework [5]. Similar to CeO<sub>2</sub>, Sm<sub>2</sub>O<sub>3</sub> also exhibits uniform nanorods, measuring approximately 20–30 nm in diameter, and a framework structure. The loose nanorod framework structure provides efficient transport of reactive gases and sufficient space for the activation of molecular oxygen, which improves catalytic performance. The Sm<sub>2</sub>O<sub>3</sub> nanorod framework shows good performance for the catalytic oxidation of CO. The 50% CO conversion temperature was approximately 280°C, and 100% CO conversion occurred at approximately 360°C.

The above results show that a reasonable precursor alloy design and a combination of dealloying and calcination processes can be used to generate nanoporous oxide structures with ideal structural parameters. These materials have favorable catalytic properties and can act as a support for noble metals or oxides, providing good conditions for the development of higher performance nanoporous materials.

## 4. Noble ligaments loaded with metallic oxides

Nanoporous composites in which the noble ligaments are loaded with metallic oxides have recently been investigated. These composites include nanoporous Ag-TiO<sub>2</sub>, Ag-CeO<sub>2</sub>, Pd-NiO, and Pd-TiO<sub>2</sub> and exhibit improved catalytic properties compared with pure nanoporous nobles. In this section, their structures and performance are reviewed.

### 4.1 Nanoporous Ag-CeO<sub>2</sub>

Nanoporous Ag-CeO<sub>2</sub> ribbons have been prepared through dealloying melt-spun Al<sub>79.5</sub>Ag<sub>20</sub>Ce<sub>0.5</sub> alloy in aqueous 5 wt% NaOH, followed by calcining in air [8]. Precursor ingots were obtained by melting the alloys composed of pure Al, Ag, and Ce. The ribbons were prepared by melt spinning at 33 m s<sup>-1</sup> and protected by 0.05 MPa Ar. The melt-spun ribbons were dealloyed in aqueous 5 wt% NaOH at room temperature. The dealloyed ribbons were calcined for 2 h at 300–700°C. The SEM analyses indicated that the morphologies were not evaluated due to the addition of Ce in the precursor alloy. However, the CeO<sub>2</sub> particles were distributed on the surface of the Ag ligaments, and a composite with CeO<sub>2</sub> loaded on the nanoporous Ag was obtained. The electrochemical tests revealed that the nanoporous Ag-CeO<sub>2</sub> catalyst exhibited enhanced activity for the direct oxidation of sodium borohydride. The Raman analysis indicated that the intensity of the peak in the 2LO band (CeO<sub>2</sub>) is stronger than that in F<sub>2g</sub> and D bands (CeO<sub>2</sub>) [8]. Therefore, the superior catalytic activity is attributed to the enhancement of the interfacial interaction between Ag and CeO<sub>2</sub>. This research provided a novel method for preparing noble metal-oxide nanocomposites with high catalytic performance. The results also indicated that the structural stability of Ag-CeO<sub>2</sub> ribbons with a homogeneous pore/grain structure is improved due to the formation of the Ag-CeO<sub>2</sub> composite. This may aid in enhancing the longevity performance.



## 4.2 Nanoporous Ag-ZrO<sub>2</sub>

After the Ag-ZrO<sub>2</sub> was prepared, nanoporous Ag-ZrO<sub>2</sub> composite catalysts were created by chemical dealloying of the melt-spun Al-Ag-Zr precursor alloys [10]. The composition of the precursor alloys was Al<sub>80-x</sub>Ag<sub>20</sub>Zr<sub>x</sub> (x = 1, 2, 3). The preparation of alloy ribbons and the dealloying method was the same as in the Ag-CeO<sub>2</sub> system. During dealloying, the zirconium (Zr) atoms released from the precursory alloys are oxidized into ZrO<sub>2</sub> and are loaded on the inner surface of the nanoporous Ag. The dealloyed ribbons exhibit an interpenetrating ligament-channel structure with nanometer-length scales. X-ray photoelectron spectroscopy (XPS) analysis indicated that the binding energy of the Zr 3d core levels decreases slightly with increasing calcination temperature because the Zr<sup>4+</sup> in the ZrO<sub>2</sub> particles is partially reduced to Zr<sup>3+</sup>, suggesting electron transfer occurring from the ZrO<sub>2</sub> to the metallic centers and the formation of oxygen vacancies in the thermal treatment. The electrochemical tests demonstrated that the current density peak increased with calcination temperature in a certain range, that nanoporous composites with the optimized ZrO<sub>2</sub> content exhibited higher catalytic activity, and that the optimized precursor alloy composition was Al<sub>78</sub>Ag<sub>20</sub>Zr<sub>2</sub>. The oxidation current density increased by 91.3% compared with that of nanoporous Ag. The excellent catalytic activity can be attributed to the interfacial interaction and electron charge transfer between Ag and ZrO<sub>2</sub>. In addition, nanoporous composites with high specific surface areas and pore volume can enhance their electrocatalytic activities, which can provide more transport channels and activity sites for conductive ions and reactant molecules.

## 4.3 Nanoporous Ag-TiO<sub>2</sub>

Nanoporous Ag-TiO<sub>2</sub> composites were prepared by dealloying the melt-spun Al-Ag-Ti ribbons in aqueous NaOH [9] in 2014. The composition of the precursor alloys was Al<sub>80-x</sub>Ag<sub>20</sub>Ti<sub>x</sub> (X = 0.5, 1, 2, 3). The preparation of alloy ribbons and the dealloying method was the same as in the Ag-CeO<sub>2</sub> and Ag-ZrO<sub>2</sub> systems. The results revealed that TiO<sub>2</sub> formed in situ on the Ag ligaments. Ti<sup>3+</sup> and Ag<sup>+</sup> species co-existed after the dealloyed samples were calcined at 600°C, which significantly influenced the catalytic oxidation of sodium borohydride. The electrochemical results showed that the nanoporous Ag-TiO<sub>2</sub> composites significantly promoted the direct oxidation of BH<sub>4</sub><sup>-</sup> superior to pure Ag. The current density of the oxidation peak for the nanoporous Ag-TiO<sub>2</sub> electrode prepared from the Al<sub>79.5</sub>Ag<sub>20</sub>Ti<sub>0.5</sub> alloy increased from 10.91 to 18.13 mA cm<sup>-2</sup>. With increasing the Ti content from 0.5 to 1.0% in the precursor alloys, the current density of the oxidation peak increased to 28.86 mA cm<sup>-2</sup>. With further increases in the Ti content, however, the current density of the nanoporous Ag-TiO<sub>2</sub> electrode obviously decreased, and the position of the oxidation peak became more positive. The enhanced catalytic activity could be attributed to the strong interfacial effects between the Ag ligaments and TiO<sub>2</sub> [9].

Among these Ag-based nanocomposites, the Ag-ZrO<sub>2</sub> nanocomposite catalyst exhibited the greatest improvement in the catalytic oxidation of sodium borohydride. The optimized precursor alloy composition was Al<sub>78</sub>Ag<sub>20</sub>Zr<sub>2</sub>. However, Ag-CeO<sub>2</sub> may have the best anti-poisoning ability of CO.

## 4.4 Nanoporous Pd-TiO<sub>2</sub>

Nanoporous Pd-TiO<sub>2</sub> composite catalysts were prepared by chemical dealloying of melt-spun Al-Pd-Ti precursor alloys [12] in 2014. The precursor alloy was Al<sub>85-x</sub>Pd<sub>15</sub>Ti<sub>x</sub> (x = 0, 0.3, 0.5, 0.7, 1.0, at%), and the preparation of alloy ribbons was the same as in the Ag-CeO<sub>2</sub> and Ag-ZrO<sub>2</sub> systems. However, calcination was

not adopted to prevent oxidation of the Pd. The structure analysis revealed that the nanoporous Pd-TiO<sub>2</sub> composites exhibited a bicontinuous interpenetrating ligament-pore structure. The XPS analysis revealed that the Pd 3d spectrum of the nanoporous Pd-TiO<sub>2</sub> composites presented a slightly negative shift to lower binding energy compared to that of nanoporous Pd. The electrochemical measurements showed that the composites observably enhanced the electrocatalytic performance toward methanol/ethanol oxidation when the Ti content in the precursor alloys was 0.3–0.7 at%. Among these composites, the nanoporous Pd-TiO<sub>2</sub> composite dealloyed from Al<sub>84.5</sub>Pd<sub>15</sub>Ti<sub>0.5</sub> exhibited the largest catalytic activity, which was triple and double that of methanol and ethanol oxidation, respectively, compared with that of nanoporous Pd. This enhancement can be attributed to the synergistic effect between Pd and TiO<sub>2</sub>. However, when the Ti content of the precursor alloys is 1 at%, the catalytic activity will obviously decline. These results imply that an electronic interaction between Pd and TiO<sub>2</sub> occurs in the nanoporous Pd-TiO<sub>2</sub> composites. The reduction of binding energy decreases the chemisorption ability of the adsorbate during electrochemical reactions. It will reduce the adsorption of CO-like intermediate species and result in superior poisoning tolerance.

#### 4.5 Nanoporous Pd-NiO

Nanoporous Pd-NiO composites were prepared for methanol oxidation in alkaline media by one-step dealloying from melt-spun Al-Pd-Ni precursor alloys [11]. The precursor alloy was Al<sub>85-x</sub>Pd<sub>15</sub>Ni<sub>x</sub> (x = 0, 0.1, 0.3, 0.5, 0.7, 1.0 at%). The preparation of alloy ribbons was the same as in the Pd-TiO<sub>2</sub> systems. The structure, morphology, composition, and electrocatalytic activities of the composites were characterized. The results demonstrated that the composites exhibited a uniform bicontinuous and interpenetrating three-dimensional nanoporous structure. Pore channels that were less than 10 nm ran throughout the ribbons. The XPS analysis revealed that the nanoporous Pd-NiO composites significantly increased compared to that of nanoporous Pd due to the reduction of the PdO content in the Pd-NiO composites. The nanoporous Pd-NiO composites possessed better electrocatalytic performance compared to that of nanoporous Pd, and the composite dealloyed from Al<sub>84.7</sub>Pd<sub>15</sub>Ni<sub>0.3</sub> showed the highest catalytic activity of the catalytic oxidation of methanol; the mass activity of the mesoporous Pd-NiO composite from Al<sub>84.7</sub>Pd<sub>15</sub>Ni<sub>0.3</sub> was 289.0 mA mg<sup>-1</sup>, which was approximately 4 times that of nanoporous Pd. The improvement in the electrocatalytic properties was attributed to the increased electrochemically active specific surface areas and the synergistic effect between Pd and NiO. The reduction of the PdO content in the nanoporous Pd-NiO composites means that there are more active sites (Pd atoms) in the composites involved in the electrocatalytic process. There is also a synergistic effect between Pd and NiO. Oxidative states of Ni in the nanoporous Pd-NiO composites serve as oxophilic sites for the oxygen source required for the surface removal of CO and promoting methanol oxidation via a surface redox process.

#### 4.6 Nanoporous Pd-ZrO<sub>2</sub>

Composition-controllable three-dimensional mesoporous Pd-ZrO<sub>2</sub> composites were synthesized through simple one-step dealloying of melt-spun Al-Pd-Zr ribbons [18]. The precursor alloy was Al<sub>85-x</sub>Pd<sub>15</sub>Zr<sub>x</sub> (x = 0, 0.5, 1, 2, 3 at%). The preparation of alloy ribbons was the same as in the Pd-TiO<sub>2</sub> systems. The Zr atoms in the precursor alloy transformed into approximately 3 nm ZrO<sub>2</sub> nanoparticles after dealloying without being calcined. The ZrO<sub>2</sub> particles embedded in the Pd ligaments. The XPS analysis revealed that the Pd 3d spectrum of the dealloyed

$\text{Al}_{83}\text{Pd}_{15}\text{Zr}_2$  sample was negatively shifted to a lower binding energy after the addition of Zr in comparison with the Pd 3d spectrum of the dealloyed  $\text{Al}_{85}\text{Pd}_{15}$ . This finding suggests the existence of electronic interactions between Pd and  $\text{ZrO}_2$ . The composites exhibited remarkable catalytic activity and stability for methanol oxidation in an alkaline electrolyte due to the synergistic effect and electronic interactions between Pd and  $\text{ZrO}_2$  [18]. Among the composites, the Pd- $\text{ZrO}_2$  sample dealloyed from the  $\text{Al}_{85}\text{Pd}_{13}\text{Zr}_2$  precursor alloy had the highest peak current density, and the mass activity of the mesoporous Pd- $\text{ZrO}_2$  composite from  $\text{Al}_{85}\text{Pd}_{13}\text{Zr}_2$  was  $254.24 \text{ mA mg}^{-1}$ , which was approximately 3.6 times that of the pure mesoporous Pd sample. In one study [18], Zr in the form of  $\text{ZrO}_2$  was embedded in the surface of the Pd ligaments in mesoporous Pd- $\text{ZrO}_2$  composites. This arrangement endowed  $\text{ZrO}_2$  with more convenient and effective absorption toward  $\text{OH}^-$  species to more rapidly transform CO-like poisoning species on the surface of the active Pd sites into carbon dioxide or other dissolvable cleansing products. The synergistic effect between Pd and  $\text{ZrO}_2$  results in more active Pd atoms being released to the surface of the samples for the use in additional methanol oxidation processes.

Among these Pd-based nanocomposites, the Pd-NiO nanocomposite catalyst showed the greatest improvement in the catalytic oxidation of methanol. The optimized precursor alloy composition was  $\text{Al}_{84.7}\text{Pd}_{15}\text{Ni}_{0.3}$ .

## 5. Nanoporous oxides loaded by noble metals

Nanoporous metal oxides have been widely applied in catalysis due to their unique porous support structure and large specific surface area, including in carbon monoxide catalytic oxidation, electrochemical catalytic oxidation of methanol, supercapacitors, and photocatalytic fields. As an intermediary, noble metals are irreplaceable in the field of catalysis. They can effectively reduce catalytic activation energy or promote electron transfer, improving the catalytic performance. Loading noble metals on oxide substrates can improve the utilization rate of noble metals and enhance the catalytic performance of oxides. Nanoporous oxides loaded or modified by noble metals can be prepared by simply dealloying melt-spun alloys and subsequent calcination in air. Nanoporous oxide materials obtained via simple and inexpensive preparation methods have homogeneously distributed pores, structural stability, large specific surface area, and excellent dispersion of supported noble metals. The large specific surface area provides more active sites for catalysis, which can effectively improve the catalytic performance of the materials. The good dispersion of loaded noble metal nanoparticles maximizes the utilization of noble metals. Typical oxide-based porous catalytic materials and catalytic applications are as follows.

### 5.1 Nanoporous CuO loaded with Au nanoparticles

Ultrafine nanoporous CuO ribbons loaded by Au nanoparticles were prepared by dealloying melt-spun Al-Cu-Au alloys and calcinating in air [4]. The precursor ingots were obtained by melting alloys composed of pure Al, Cu, and Au. The ribbons were prepared by melt spinning at  $33 \text{ m s}^{-1}$  and protected by 0.05 MPa Ar. The as-quenched ribbons were immersed in aqueous 5 wt% NaOH at room temperature. The dealloyed samples were rinsed with reverse osmosis water and dehydrated alcohol. The dealloyed ribbons were calcined in a muffle furnace at 300–900°C for 1 h.

The formation mechanism of the nanoporous Au-CuO composites is as follows: after the Al-Cu-Au alloys are immersed in NaOH solutions, Al is preferentially etched, and the released Cu atoms in the dealloyed layer are rearranged to form a



nanoporous structure. The Cu and Au atoms are released simultaneously because the Au atoms are mainly dissolved in the fcc Al. A Cu (Au) solid solution forms due to the existence of unlimited solid solution between Au and Cu according to the Cu-Au binary phase diagram. After the samples are calcined in air, Cu ligaments are oxidized to CuO, and the phase segregation occurs because the Au cannot be dissolved by CuO. During calcination, Au atoms diffuse to the surface of the CuO layers and form Au clusters. With the absorbed O atoms diffusing to the inner Cu and Cu<sub>2</sub>O, the Au atoms dissolved in the Cu solution diffuse to the Au clusters and form Au particles, leading to a slight growth of Au particles. As a result, a portion of Au particles emboss from the surface of CuO ligaments, where the as-generated Au nanoparticles are partially embedded in CuO ligaments. Due to the unique porous structure, Au nanoparticles are immobilized on the surface of the ligaments, and the aggregation of particles can be effectively prevented.

The experimental [4] results indicate that the composites have large surface areas and high activity and stability. The CO conversion as a function of reaction temperature for the dealloyed Al<sub>79.7</sub>Cu<sub>20</sub>Au<sub>0.3</sub> ribbons calcined at different temperatures indicated that the CO conversion rate can reach 100.0% at 180°C for samples treated with the optimized process. The X-ray photoelectron spectroscopy (XPS) results indicate that the superior performance at low temperature is ascribed to the presence of Au<sup>+1</sup> species and the interfacial interaction between Au nanoparticles and CuO ligaments. The binding energy of Cu 2p in the catalyst prepared from Al<sub>79.7</sub>Cu<sub>20</sub>Au<sub>0.3</sub> alloy shifts lower due to an interaction between Au and CuO<sub>x</sub>. Notably, Au<sup>+1</sup> is present on the surface of the CuO, which acts as an active site for CO oxidation and can lead to more activated CO than Au<sup>0</sup>. The catalytic measurement showed that the valence of Au changes whereas the valence of Cu does not change, indicating that the Au state is vital to maintaining a high CO conversion rate and long-term stability. It is probable that Au and Au<sup>+1</sup> sites located at the interface enhance the absorption of CO and O and that the presence of Cu<sup>2+</sup> would result in high mobility and reactivity of surface lattice oxygen to participate in the reaction, which are favorable to the catalytic reaction of CO oxidation.

## 5.2 CeO<sub>2</sub> nanorod framework loaded with Au

CeO<sub>2</sub> nanorod frameworks (NFs) with the porous structure loaded with Au were prepared by dealloying melt-spun Al<sub>89.7</sub>Ce<sub>10</sub>Au<sub>0.3</sub> ribbons and calcination [14]. The preparation of alloy ribbons was the same as that in the Au-CuO system. The as-quenched ribbons were immersed in aqueous 20 wt% NaOH at a room temperature for 2 h and treated at 80°C for 10 h. The dealloyed ribbons were pretreated at 200–800°C for 2 h in pure O<sub>2</sub>. After the dealloyed sample was calcined at 400°C in O<sub>2</sub>, the XPS results demonstrated that the Au peaks slightly shifted lower due to the interaction of gold with oxygen vacancies. This phenomenon indicates that Au species interacted with the CeO<sub>2</sub> nanorods via charge transfer between Au and CeO<sub>2</sub>. The Au<sup>δ+</sup>/Au<sup>0</sup> ratio of calcined Au-CeO<sub>2</sub> (0.39) was much higher than that of the dealloyed sample (0.21). Therefore, Au<sup>0</sup> and Au<sup>δ+</sup> species coexisted in the calcined Au-CeO<sub>2</sub> due to strong interactions, which can effectively enhance the catalytic activity. The Au-CeO<sub>2</sub> nanorod catalyst calcined at 400°C exhibited much higher catalytic activity for CO oxidation than the dealloyed sample or pure CeO<sub>2</sub> nanorods [14]. Moreover, its complete reaction temperature was as low as 91°C. The designed Au-CeO<sub>2</sub> catalyst possessed extreme sintering resistance and exhibited high performance due to the enhanced interaction between the Au clusters/NPs and CeO<sub>2</sub> nanorods during calcination. The CeO<sub>2</sub> nanorod framework structure can be retained, and some Au nanoparticles supported on the nanorod CeO<sub>2</sub> surfaces did not evolve after catalytic testing.



The formation process of the Au-CeO<sub>2</sub> nanorod catalyst can be deduced as: during the formation of the porous CeO<sub>x</sub> framework, the Au atoms may mix with the nanorods. After the nanorods are calcined in O<sub>2</sub>, CeO<sub>x</sub> is oxidized to CeO<sub>2</sub> NF, whereas the Au atoms diffuse to the surface of the nanorods and form NPs/clusters or nanoparticles, which are in situ supported and immobilized on the surface of the CeO<sub>2</sub> nanorods. The dispersion of Au NPs or clusters on CeO<sub>2</sub> NF could create many nanoscale contact interfaces and prevent NP/cluster sintering and migration of active Au species during calcination and catalytic reaction. This result was significantly different from those of other preparation methods, in which the NP aggregation typically leads to unexpected activity loss due to the collapse of the nanostructure during the annealing and catalytic processes.

### 5.3 Nanoporous Pt-TiO<sub>2</sub> nanocomposites

Nanoporous TiO<sub>2</sub> and Pt-TiO<sub>2</sub> composites were prepared by dealloying melt-spun Al-Si-Ti and Al-Si-Ti-Pt alloys, respectively [16]. The preparation of alloy ribbons was the same as in the Au-CuO system. The as-quenched ribbons were dealloyed in aqueous 10 wt% NaOH at 80°C. After the samples were dried in air, the ribbons were immersed in aqueous 3 wt% HCl at an ambient temperature for 7 h. The samples were then calcined at 400°C for 2 h. The mechanism of formation of the structure is as follows: Al and Si are etched away in the NaOH solution, and Ti and Pt are retained. During dissolution, the remaining Ti and Pt move freely along the interface between the alloy and the dissolution medium. The Ti reacts with NaOH to form insoluble Na-titanate ( $\text{Ti} + \text{NaOH} \rightarrow \text{Na-titanate}$ ). The Pt-Na-titanate reorganizes into a three-dimensional network exhibiting an open porosity. After acid treatment, there is no significant evolution in the microstructure morphology in the H-titanate ( $\text{Pt-Na-titanate} + \text{H}^+ \rightarrow \text{Pt-H-titanate} + \text{Na}^+$ ). Nanoporous Pt-TiO<sub>2</sub> can be obtained through the calcination of Pt-H-titanate. Measurement of the structural parameters indicated that the nanoporous Pt-TiO<sub>2</sub> nanocomposites exhibit large specific surface areas, small pore diameters, and large pore volumes.

The performance measurements revealed that nanoporous TiO<sub>2</sub> showed favorable photocatalytic performance in the degradation of methyl orange (MO). Using Pt-TiO<sub>2</sub> nanocomposites, approximately 98% of the MO solution degraded in 50 minutes. The significant enhancement of the photocatalytic performance of Pt-TiO<sub>2</sub> was a result of the large specific surface area of approximately 98.06 m<sup>2</sup> g<sup>-1</sup> and synergistic effect between TiO<sub>2</sub> and metallic Pt, which reduced the band gap of TiO<sub>2</sub> and expanded the absorption range. With a high work function, Pt enhances the Schottky barrier effect; the Schottky barrier formation at the interfaces of Pt-TiO<sub>2</sub> composites reduced the rate of electron-hole (e-h<sup>+</sup>) pair recombination, which contributed to the improvement of the photocatalytic performance.

Noble metal-modified nanoporous oxides prepared by the dealloying method and their supported noble metals have the following advantages: (1) unique stable structure, which results in stability of the catalyst, (2) refined and homogeneous distribution of nanopores provides a larger specific surface area for the catalyst, exposing more active sites and effectively promoting catalytic performance, (3) loaded noble metals avoid agglomeration and evenly disperse on oxide surfaces or ligaments, which improves the availability of noble metals and enhances catalytic performance, and (4) the tight interaction between the supported noble metal and the oxide enhances the synergy between the noble metal and the oxide.

## 6. Conclusions

By the reasonable design of precursors and adoption of dealloying process, the nanoporous oxides, such as CuO, NiO, TiO<sub>2</sub>, Co<sub>3</sub>O<sub>4</sub>, and CeO<sub>2</sub>, noble-metal-based nanoporous composites, such as Ag ligaments loaded with CeO<sub>2</sub>, TiO<sub>2</sub>, ZrO<sub>2</sub>, or NiO, and Pd ligaments loaded with TiO<sub>2</sub> or ZrO<sub>2</sub> could be obtained. Adding the noble into the melt-spun Al-M (M = Ce, Cu, and Ti) ribbons and dealloying in NaOH or KOH solutions, oxide-based nanoporous composites, such as Au loaded on CuO and CeO<sub>2</sub> or Pt loaded on TiO<sub>2</sub>, have been achieved. The catalytic performances of the noble-based nanoporous composites, including the catalytic oxidation of methanol and ethanol, could be improved obviously comparing with single nanoporous nobles. The catalytic oxidation activities of CO for the oxide-based nanoporous composites have also been increased much. The rare earth elements could play an important role in the nanoporous materials. Sometimes, they could be the key metals for the nanoporous composites with high properties.

## Acknowledgements


This work was supported by the National Natural Science Foundation of China (Grant no. 51371135, 51771141). The authors of this chapter thank G.J. Li, Y.Y. Song, and X.L. Zhang for their contributions.

## Author details

Dong Duan, Haiyang Wang, Wenyu Shi and Zhanbo Sun\*  
School of Science, Xi'an Jiaotong University, Xi'an, P.R. China

\*Address all correspondence to: [szb@mail.xjtu.edu.cn](mailto:szb@mail.xjtu.edu.cn)

## IntechOpen

© 2018 The Author(s). Licensee IntechOpen. This chapter is distributed under the terms of the Creative Commons Attribution License (<http://creativecommons.org/licenses/by/3.0>), which permits unrestricted use, distribution, and reproduction in any medium, provided the original work is properly cited. 

## References

- [1] Wittstock A, Zielasek V, Biener J, et al. Nanoporous gold catalysts for selective gas-phase oxidative coupling of methanol at low temperature. *Science*. 2010;**327**(5963):319-322. DOI: 10.1126/science.1183591
- [2] Chen A, Holt-Hindle P. Platinum-based nanostructured materials: Synthesis, properties, and applications. *Chemical Reviews*. 2010;**110**(6):3767-3804. DOI: 10.1021/cr9003902
- [3] Kou T, Jin C, Zhang C, et al. Nanoporous core-shell Cu@Cu<sub>2</sub>O nanocomposites with superior photocatalytic properties towards the degradation of methyl orange. *RSC Advances*. 2012;**2**(33):12636-12643. DOI: 10.1039/c2ra21821f
- [4] Zhang X, Li G, Yang S, Song X, Sun Z. Nanoporous CuO ribbons modified by Au nanoparticles through chemical dealloying and calcination for CO oxidation. *Microporous and Mesoporous Materials*. 2016;**226**:61-70. DOI: 10.1016/j.micromeso.2015.12.028
- [5] Zhang X, Li K, Shi W, Wei C, Song X, Yang S, et al. Baize-like CeO<sub>2</sub> and NiO/CeO<sub>2</sub> nanorod catalysts prepared by dealloying for CO oxidation. *Nanotechnology*. 2017;**28**(4):045602. DOI: 10.1088/1361-6528/28/4/045602
- [6] Zhang X, Li G, Song X, Yang S, Sun Z. Three-dimensional architecture of Ag/CeO<sub>2</sub> nanorod composites prepared by dealloying and their electrocatalytic performance. *RSC Advances*. 2017;**7**(52):32442-32451. DOI: 10.1039/c7ra04651k
- [7] Tauster SJ, Fung SC, Garten RL. Strong metal-support interactions. Group 8 noble metals supported on titanium dioxide. *Journal of the American Chemical Society*. 1978;**100**(1):170-175. DOI: 10.1021/ja00469a029
- [8] Guijing L, Feifei L, Xin W, Xiaoping S, Zhanbo S, Zhimao Y, et al. Nanoporous Ag-CeO<sub>2</sub> ribbons prepared by chemical dealloying and their electrocatalytic properties. *Journal of Materials Chemistry A*. 2013;**1**(16):4974-4981. DOI: 10.1039/c3ta01506h
- [9] Li G, Sun Z, Zhang X, Song X, Sun Z, Feng W. Preparation of nanoporous Ag@TiO<sub>2</sub> ribbons through dealloying and their electrocatalytic properties. *Journal of Solid State Electrochemistry*. 2015;**19**(4):967-974. DOI: 10.1007/s10008-014-2702-x
- [10] Zhang X, Wei C, Song Y, Song X, Sun Z. Nanoporous Ag-ZrO<sub>2</sub> composites prepared by chemical dealloying for borohydride electro-oxidation. *International Journal of Hydrogen Energy*. 2014;**39**(28):15646-15655. DOI: 10.1016/j.ijhydene.2014.07.102
- [11] Song Y, Zhang X, Yang S, Wei X, Sun Z. Electrocatalytic performance for methanol oxidation on nanoporous Pd/NiO composites prepared by one-step dealloying. *Fuel*. 2016;**181**:269-276. DOI: 10.1016/j.fuel.2016.04.086
- [12] Yanyan S, Caihua W, Xiaolong Z, Xin W, Xiaoping S, Zhanbo S. Nanoporous Pd/TiO<sub>2</sub> composites prepared by one-step dealloying and their electrocatalytic performance for methanol/ethanol oxidation. *Materials Chemistry and Physics*. 2015;**161**:153-161. DOI: 10.1016/j.matchemphys.2015.05.030
- [13] Duan D, Hao C, Shi W, Wang H, Sun Z. Sm<sub>2</sub>O<sub>3</sub>/Co<sub>3</sub>O<sub>4</sub> catalysts prepared by dealloying for low-temperature CO oxidation. *RSC Advances*. 2018;**8**(21):11289-11295. DOI: 10.1039/C8RA01219A
- [14] Zhang X, Duan D, Li G, Feng W, Yang S, Sun Z. Monolithic Au/CeO<sub>2</sub>

nanorod framework catalyst prepared by dealloying for low-temperature CO oxidation. *Nanotechnology*. 2018;**29**(9):095606. DOI: 10.1088/1361-6528/aaa726

[15] Li G, Song X, Lu F, Sun Z, Yang Z, Yang S, et al. Formation and control of nanoporous Ag through electrochemical dealloying of the melt-spun Cu-Ag-Ce alloys. *Journal of Materials Research*. 2012;**27**(12):1612-1620. DOI: 10.1557/jmr.2012.121

[16] Shi W, Song Y, Zhang X, Duan D, Wang H, Sun Z. Nanoporous Pt/TiO<sub>2</sub> nanocomposites with greatly enhanced photocatalytic performance. *Journal of the Chinese Chemical Society*. Nov. 5, 2018. DOI: 10.1002/jccs.201700251

[17] Xu C, Liu Y, Zhou C, Wang L, Geng PH, Ding PY. An in situ dealloying and oxidation route to Co<sub>3</sub>O<sub>4</sub> nanosheets and their ambient-temperature CO oxidation activity. *ChemCatChem*. 2011;**3**:399-407. DOI: 10.1002/cctc.201000275

[18] Song Y, Duan D, Shi W, Wang H, Yang S, Sun Z. Promotion effects of ZrO<sub>2</sub> on mesoporous Pd prepared by a one-step dealloying method for methanol oxidation in an alkaline electrolyte. *Journal of the Electrochemical Society*. 2017;**164**:F1495-FF505. DOI: 10.1149/2.1821713jes

[19] Zhang X, Li G, Duan D, Wang H, Sun Z. Formation and control of nanoporous Pt ribbons by two-step dealloying for methanol electro-oxidation. *Corrosion Science*. 2018;**135**:57-66. DOI: 10.1016/j.corsci.2018.02.030

[20] Ganduglia-Pirovano MV, Hofmann A, Sauer J. Oxygen vacancies in transition metal and rare earth oxides: Current state of understanding and remaining challenges. *Surface Science Reports*. 2007;**62**:219-270. DOI: 10.1016/j.surfrep.2007.03.002

[21] Guo X, Zhou R. A new insight into morphology effect of ceria on CuO/CeO<sub>2</sub> catalysts for CO selective oxidation in hydrogen-rich gas. *Catalysis Science & Technology*. 2016;**6**:3862-3871. DOI: 10.1039/C5CY01816A

[22] Maitarad P, Han J, Zhang D, Shi L, Namuangruk S, Rungrotmongkol T. Structure-activity relationships of NiO on CeO<sub>2</sub> nanorods for the selective catalytic reduction of NO with NH<sub>3</sub>: Experimental and DFT studies. *Journal of Physical Chemistry C*. 2014;**118**:9612-9620. DOI: 10.1021/jp5024845

[23] Lin Z, Li X, Yao Z, Chen Z, Mei H, Zhu R, et al. transition-metal doped ceria microspheres with nanoporous structures for CO oxidation. *Scientific Reports*. 2016;**6**:23900. DOI: 10.1038/srep23900

[24] Liu S, Yu J, Jaroniec M. Anatase TiO<sub>2</sub> with dominant high-energy {001} facets: Synthesis, properties, and applications. *Chemistry of Materials*. 2011;**23**(18):4085-4093. DOI: 10.1021/cm200597m

[25] Ong WJ, Tan LL, Chai SP, Yong ST, Mohamed AR. Highly reactive {001} facets of TiO<sub>2</sub>-based composites: Synthesis, formation mechanism and characterization. *Nanoscale*. 2014;**6**:1946-2008. DOI: 10.1039/c3nr04655a

[26] Zhao W, Sun Y, Castellano FN. Visible-light induced water detoxification catalyzed by PtII dye sensitized titania. *Journal of the American Chemical Society*. 2008;**130**:12566-12567. DOI: 10.1021/ja803522v

[27] Li R, Chan KC, Liu XJ, Zhang XH, Liu L, Li T, et al. Synthesis of well-aligned CuO nanowire array integrated with nanoporous CuO network for oxidative degradation of methylene blue. *Corrosion Science*. 2017;**126**:37-43. DOI: 10.1016/j.corsci.2017.06.001



- [28] Liang K, Tang X, Wei B, Hu W. Fabrication and characterization of a nanoporous NiO film with high specific energy and power via an electrochemical dealloying approach. *Materials Research Bulletin*. 2013;**48**:3829-3833. DOI: 10.1016/j.materresbull.2013.05.086
- [29] Li S, Zhu H, Qin Z, Wang G, Zhang Y, Wu Z, et al. Morphologic effects of nano CeO<sub>2</sub>—TiO<sub>2</sub> on the performance of Au/CeO<sub>2</sub>—TiO<sub>2</sub> catalysts in low-temperature CO oxidation. *Applied Catalysis B: Environmental*. 2014;**144**:498-506. DOI: 10.1016/j.apcatb.2013.07.049
- [30] Kim HY, Lee HM, Henkelman G. CO oxidation mechanism on CeO<sub>2</sub>-supported Au nanoparticles. *Journal of the American Chemical Society*. 2012;**134**:1560-1570. DOI: 10.1021/ja207510v
- [31] Yang S, Zhu W, Wang J, Chen Z. Catalytic wet air oxidation of phenol over CeO<sub>2</sub>—TiO<sub>2</sub> catalyst in the batch reactor and the packed-bed reactor. *Journal of Hazardous Materials*. 2008;**153**:1248-1253. DOI: 10.1016/j.jhazmat.2007.09.084
- [32] Huang PX, Wu F, Zhu BL, Gao XP, Zhu HY, Yan TY, et al. CeO<sub>2</sub> nanorods and gold nanocrystals supported on CeO<sub>2</sub> nanorods as catalyst. *Journal of Physical Chemistry B*. 2005;**109**:19169-19174. DOI: 10.1021/jp052978u
- [33] Wang H, Liang M, Zhang X, Duan D, Shi W, Song Y, et al. Novel CeO<sub>2</sub> nanorod framework prepared by dealloying for supercapacitors applications. *Ionics*. 2018;**24**:2063-2072. DOI: 10.1007/s11581-018-2443-4